

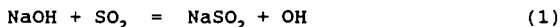
THE CHEMISTRY OF SODIUM WITH SULFUR IN FLAMES

Martin Steinberg and Keith Schofield
Quantum Institute
University of California
Santa Barbara, CA 93106

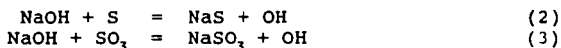
INTRODUCTION

The use of fuel/air systems contaminated with sodium and sulfur in combustion driven gas turbines is a source of turbine blade corrosion. Sodium sulfate, which deposits on turbine surfaces or is chemically formed there, has long been recognized as the active corrosive agent.^{1,2} There is very little chemical kinetic information for modeling this practical problem, and one is forced to invoke chemical equilibrium to attempt any quantitative treatment.

Sodium/sulfur chemistry has been addressed in a very few studies. Fenimore³ reported a decrease of Na with the addition of SO₂ to rich and lean H₂/Air flames which he attributed to the equilibration of Reaction (1).



Durie *et al*⁴, in a study in rich and lean C₃H₈/O₂/N₂ flames assigned the observed Na decay with sulfur addition to the equilibration of Reactions (2) and (3), respectively.



They also felt that Fenimore's data supported their model. In a mass spectrometric study in a lean CH₄/Air flame, Fryburg *et al*⁵ identified NaSO₂, NaSO₃, and Na₂SO₄ as gas phase products in lean methane-oxygen flames. They reported clogging of their sampler inlet orifice which limited their data gathering. In fact, it is not possible to conclude whether the observed species are homogeneous gas phase products, or are formed heterogeneously in the sample inlet probe.

The present study is an outgrowth of two previous efforts in this laboratory, sulfur chemistry⁶ and sodium oxidation chemistry⁷, in H₂/O₂/N₂ flames. Sodium/sulfur chemistry competes with the sodium oxidation chemistry and both are influenced by the flame radical/sulfur chemistry interaction. A brief overview follows.

The radicals H, O, and OH in the hot burnt gases of H₂/O₂/N₂ flames sharply overshoot their equilibrium levels through rapid bimolecular chain Reactions (4-6)



which are balanced due to their large kinetic fluxes in an otherwise non-equilibrated environment. Thus from measures of OH and temperature the concentrations of H, O, OH, and O₂ in rich or H₂ in lean flames

are calculable. The radicals recombine through slow 3-body reactions. With the addition of sulfur to these flames, radical recombination is catalyzed and in turn the radicals establish balances between SO_2 , SO , H_2S , SH , S_2 , and S . As with the flame radicals, the concentrations of these sulfur species also can be determined from measures of OH and T and the total sulfur content. SO_3 is formed in the slow termolecular Reaction 7.



It can be assumed to be in steady state through Reaction 7 followed by reactions of SO_3 with H and O regenerating SO_2 .

The oxidation of sodium in lean, sulfur free, $\text{H}_2/\text{O}_2/\text{N}_2$ flames was found to exhibit an interesting chemistry.⁷ The dominant oxidation path occurs through a fast 3-body process



and the NaO_2 then reacts with the radicals to produce overshoots in NaOH concentrations, which are balanced with small amounts of NaO. A kinetic model was developed for this system from which the concentration profiles of Na, NaO_2 , NaOH, and Na are determined from measures of OH and T and the total sodium concentration. The sodium/sulfur interaction is imbedded in this complex but reasonably understood environment.

EXPERIMENTAL CONDITIONS

Measurements are made in the laminar, premixed, one dimensional flow in the post flame gases above a Padley-Sugden⁸ burner of bundled hypodermic tubing with an overall diameter of 2.2 cm. Sodium is introduced as an aqueous NaNO_3 aerosol generated in an ultrasonic nebulizer⁹ and transported by a portion of the gas flow to the burner. Sulfur is added as H_2S and SO_2 to rich and lean flames, respectively, to minimize thermal contributions these additives make to flame properties. A schematic of the optical system is shown in Figure 1. Temperatures are measured using the sodium line reversal method. Sodium and OH are measured by laser induced fluorescence^{10,11} using a YAG pumped dye laser source beam passed through the flame parallel to the burner surface. The fluorescence, from a slice of the laser excited flame volume is collected by a 6 inch mirror, passed through an image rotator, and focused into the vertical entrance slit of the monochromator. The burner is mounted on a motor driven table programmed to collect data as a function of distance (and time) above the burner surface. The monochromator output is detected with a photomultiplier, the signal amplified, processed in a boxcar integrator, and recorded.

One line of the sodium doublet at 589.0 nm was pumped with fluorescence detection at 589.6 nm. Saturation excitation was employed to eliminate quenching uncertainties. The $\text{OH}(\text{A}^2\Sigma^+ - \text{X}^2\Pi)$ (1,0), $\text{R}_1(6)$ transition was excited at 281.14 nm and fluorescence detected at 314.69 nm from the (1,1), $\text{Q}_1(7)$ transition. The OH measurements are absolute values calibrated against a high temperature flame in which OH is at thermodynamic equilibrium.¹²

RESULTS

Measurements of temperature, OH, and Na have been made in 10-lean and 9-rich $H_2/O_2/N_2$ flames containing sodium with and without added sulfur. The flame matrix is listed in Table 1. Measured (Na) and (OH) profiles are plotted for a lean flame in Figure 2. It should be noted that the decreases in (Na) with added SO_2 result from two effects. The first may be the formation of some Na/S compound. The second, which is dominant in lean flames, is the increased sodium oxidation resulting from the sulfur catalyzed flame radical decay. It is this interaction that complicates the analysis.

KINETIC MODELING

The sodium experimental data has been scaled to refer to the same amount of total sodium in each flame. Sodium concentrations are the order of 10^{11} cm^{-3} , the radicals at least a few orders of magnitude greater, with total sulfur at the 1 to 2% level. Thus all species can influence (Na) but sodium has no effect on other species concentrations.

Checks on the balanced chemistry of Reactions (1-3), suggested by Fenimore³ and Durie *et al*⁴, indicated no such equilibrations. Plots of $\log K$ against T^{-1} for each of the reactions did not correlate the data. Apparently the chemistry is more complicated, requiring kinetic modeling.

With no sulfur present, the total sodium concentration, $(Na)_T$, is given by Equation 9, and with sulfur by Equation 10.

$$(Na)_T = (Na)_0 + (NaO_2)_0 + (NaOH)_0 + (NaO)_0 \quad (9)$$

$$(Na)_T = (Na)_s + (NaO_2)_s + (NaOH)_s + (NaO)_s + (NaX) \quad (10)$$

The subscript "s" indicates the presence of sulfur and (NaX) is a sodium/sulfur compound. To begin the analysis we will assume the formation of a single, dominant NaX. Eliminating $(Na)_T$, we obtain Equation (11)

$$(Na)_s = \frac{(1 + x + y + z)_0}{(1 + x + y + z + w)_s} (Na)_0 \quad (11)$$

where $x = (NaO_2)/(Na)$, $y = (NaOH)/(Na)$, $z = (NaO)/(Na)$, and $w = (NaX)/(Na)$. Equation (11) relates the sodium concentrations with and without sulfur at corresponding times in the profiles for a given flame. The parameter $(1 + x + y + z)_0$ is calculated using the oxidation model for the sulfur free flames. We have used Equation (11) to calculate the values for $(Na)_s$ from the experimental values for corresponding $(Na)_0$ in the sulfur free flames. The parameter $(1 + x + y + z + w)_s$ is modeled to achieve a comparison between the so calculated $(Na)_s$ values and those observed experimentally.

A list of possible reactions have been written for the production and consumption of $NaSO$, $NaSO_2$, $NaSO_3$, $NaSH$, NaS , and NaS_2 . At the sodium levels in this study there is little chance for the formation of any disodium compounds, such as Na_2SO_4 . Vibrational frequencies

and bond lengths have been estimated for calculating thermodynamic properties of the sodium/sulfur species.¹³ Estimates have been made for the gas kinetic collision rates of all the bimolecular reactions. Forward and reverse rate constants, related through the calculated equilibrium constants, have been formulated with the dissociation energy, $D_0(\text{NaX})$, for each of the assumed NaX products, as a parameter to be determined in the modeling program.

(NaO_2), (NaOH), (NaO), and (NaX) in the sulfur bearing flames were determined using a steady state analysis for these species. Three body rate constants for sodium with sulfur species were set initially equal to the rate constants for the sodium-oxygen analogs. Values for $D_0(\text{Na-X})$ and attenuating multipliers for each rate constant were then adjusted to achieve an optimal fit between calculated and experimental values for (Na)_s.

A reaction scheme for NaSO, added to the sodium oxidation model is seen in Figure 3. A comparison of the calculated and experimental profiles for (Na)_s are plotted in Figure 4. The optimal conditions required only reactions (21), (23), and (24) from Figure 3. All the remaining sodium/sulfur processes have negligible influence. NaSO and NaO_2 are isoelectronic and it was assumed that the termolecular formation rate constants for NaSO and NaO_2 are equal. The model yielded a value for $D_0(\text{Na-SO}) = 70$ kcal/mole. NaSO concentrations varied from about 1 to 24% of the total sodium in the rich flames with lower temperatures favoring the higher concentrations. NaOH concentrations ranged from about 1 to 16% with the higher concentrations favored in the high temperature flames. There appears to be little coupling of the sodium sulfidation and oxidation chemistries. Application of the NaSO model to the lean $\text{H}_2/\text{O}_2/\text{N}_2$ flames only made a small contribution to that chemistry.

Similar analyses have been conducted in the rich flames assuming NaS, NaS_2 , and NaSH as the primary sodium/sulfur product. NaS modeling does not quite approach the performance of the NaSO model. In addition the NaS optimal conditions require a value for $D_0(\text{Na-SO}) = 81$ kcal/mole, about 25 kcal/mole too large, ruling out NaS as a dominant product. NaSH and NaS_2 exhibit poorer accommodations to the experimental data.

Only NaSO, and NaSO_2 are possible candidates in the lean flames. NaSO_2 was ruled out as a meaningful product primarily due to the very low SO_2 steady state concentrations. NaSO_2 has been examined as a dominant product in both the rich and lean flames. Optimal rich flame conditions for NaSO_2 required $D_0(\text{Na-SO}) = 70$ kcal/mole. When applied to the lean flames this model consumed far too much sodium. Modeling NaSO, in the lean flames gave a very good approximation to the experimental data with a value for $D_0(\text{Na-SO}) = 46$ kcal/mole. The application to the lean flame data in Figure 2 is seen in Figure 5. In the lean flames NaSO levels reach a maximum of only about 0.5% of the total sodium. The higher values are favored in the richer and cooler flames. NaOH accounts for 8 to 70% of the total sodium with higher values in the leaner flames. It does appear, however, that there is some increased NaOH formation occurring through the small but effective NaSO_2 intermediate. In the rich flame this NaSO_2 model makes a small, almost negligible contribution.

CONCLUSIONS

The sodium/sulfur chemistry has been modeled in a series of rich and lean $H_2/O_2/N_2$ flames. It was found that simple equilibria identified in earlier studies can not account for the behavior exhibited in the present data. Kinetic modeling has been conducted assuming, as is often the case, that one sodium/sulfur product may dominate. To a good approximation this seems to be the situation in both the rich and lean flames. NaSO appears to be the dominant sodium/sulfur product in the rich $H_2/O_2/N_2$ flames with NaSO₂ dominant in the lean flames.

The conclusions drawn for the lean flames are fairly firm. NaSO₂ is the only viable sodium/sulfur product in this oxidizing environment. However, we must view the rich flame discussion as provisional. It is possible that some combination of NaSO with NaSO₂, or even NaS or NaSH can provide a better description of the rich flame behavior. Currently, these combinations of contributing sodium/sulfur products are being examined.

ACKNOWLEDGEMENT

The support of this work by the Department of Energy, Morgantown Energy Technology Center under Grant DE-FG21-86MC23135 is gratefully acknowledged.

REFERENCES

1. E.L. Simons, G.V. Browning, and H.A. Liebafsky, *Corrosion*, **11**, 505t (1955).
2. M.A. DeCrescente and N.S. Bornstein, *Corrosion*, **24**, 127 (1968).
3. C.P. Fenimore, *Symp. (Int.) on Combustion*, **14**, 955 (1973).
4. R.A. Durie, G.M. Johnson, and M.Y. Smith, *Symp. (Int.) on Combustion*, **15**, 1123 (1975).
5. G.C. Fryburg, R.A. Miller, C.A. Stearns, and F.J. Kohl, in "High Temperature Metal Halide Chemistry," D.L. Hildenbrand and D.D. Cubicciotti, Editors, p. 468, The Electrochemical Society Softbound Proceedings Volume 78-1, Princeton, NJ (1978); also NASA TM-73794 (1977).
6. C.H. Muller, K. Schofield, M. Steinberg, and H.P. Broida, *Symp. (Int.) on Combustion*, **17**, 867, (1979).
7. J.T. Hynes, M. Steinberg, and K. Schofield, *J. Chem. Phys.* **80**, 2585 (1984).
8. P.J. Padley and T.M. Sugden, *Proc. Roy. Soc. London Ser. A*, **248**, 248 (1958).
9. M.B. Denton and D.B. Swartz, *Rev. Sci. Instrum.* **45**, 81 (1974).
10. K. Schofield and M. Steinberg, *Opt. Eng.* **20**, 501 (1981).
11. J.T. Hynes, M. Steinberg, and K. Schofield, *J. Chem. Phys.* **80**, 2585 (1984).
12. C.H. Muller III, K. Schofield, and M. Steinberg, *ACS Symp. Series*, **134**, 103 (1980).
13. B.J. McBride and S. Gordon, "Fortran IV Program for Calculation of Thermodynamic Data," NASA TN D-4097, August, 1967 (Updated version).

Table 1. Experimental Hydrogen/Oxygen/Nitrogen Flame Matrix and Properties.

H ₂ /O ₂ /N ₂	Temperature (K)	[H ₂ O]	[O ₂] (molecules/cm ³)	[H ₂]	[OH]
0.6/1/1	1906-1929	1.0(18)	1.2(18)	---	3.8->0.7(16) ^a
1/1/2	2066-2100	9.9(17)	4.8(17)	---	3.8->1.1(16)
1/1/3	1667-1730	9.5(17)	4.7(17)	---	3.7->0.3(16)
1.4/1/3	2125-2197	9.8(17)	2.0(17)	---	3.5->1.4(16)
1.4/1/4	1810-1847	9.8(17)	2.1(17)	---	3.6->0.5(16)
1.4/1/5	1654-1669	9.3(17)	2.0(17)	---	3.6->0.3(16)
1.8/1/3	2280-2405	1.1(18)	5.9(16)	---	4.0->1.9(16)
1.8/1/4	2060-2228	9.8(17)	5.1(16)	---	3.6->1.4(16)
1.8/1/5	1825-1916	1.0(18)	5.3(16)	---	3.2->0.7(16)
1.8/1/6	1695-1726	9.6(17)	5.2(16)	---	3.1->0.4(16)
2.2/1/4	2160-2308	1.0(18)	---	1.1(17)	3.8->1.3(16)
2.2/1/5	1975-2106	9.7(17)	---	9.8(16)	2.7->0.8(16)
2.2/1/6	1780-1897	9.4(17)	---	9.4(16)	1.9->0.5(16)
3/1/4	2050-2167	9.7(17)	---	5.5(17)	2.4->0.3(16)
3/1/5	1883-2010	9.1(17)	---	4.6(17)	1.2->0.2(16)
3/1/6	1775-1857	8.8(17)	---	4.4(17)	1.1->0.2(16)
4/1/4	1898-2042	9.1(17)	---	9.1(17)	1.0->0.2(16)
4/1/5	1767-1900	8.6(17)	---	8.7(17)	0.6->0.1(16)
4/1/6	1650-1788	8.2(17)	---	8.2(17)	0.6->0.1(16)

^aConcentrations, read as 3.8×10^{16} near the flame reaction zone decaying downstream to 0.7×10^{16} at 4.0 ms.

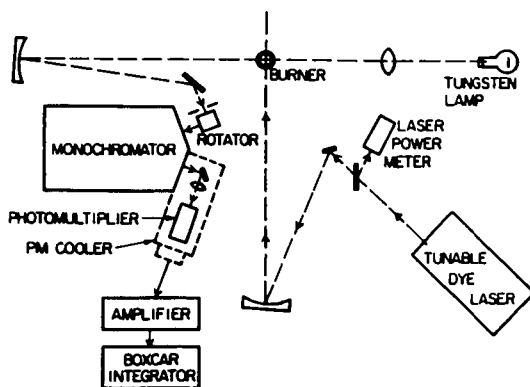


Figure 1. Optical Arrangement

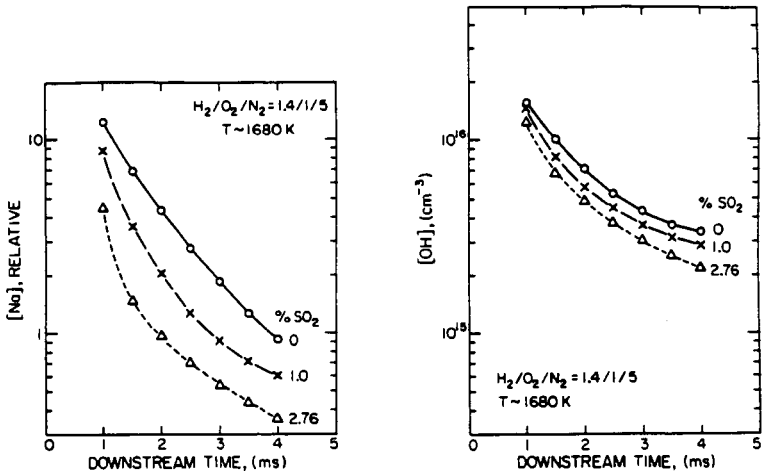


Figure 2. Measured (Na) and (OH) profiles in lean $H_2/O_2/N_2$ flames with varying amounts of SO_2 .

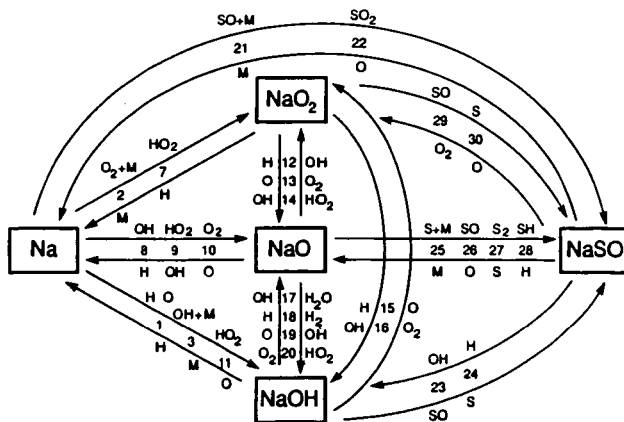


Figure 3. Sodium/sulfur reaction scheme assuming that $NaSO$ is the dominant sodium/sulfur product.

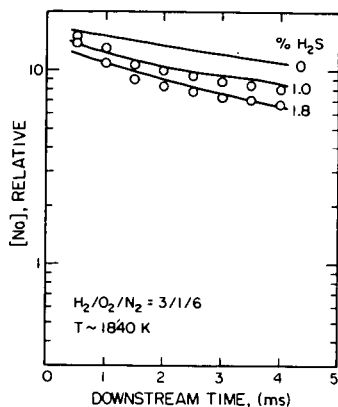


Figure 4. Comparison of measured and calculated sodium profiles in rich $H_2/O_2/N_2$ flames with varying H_2S and $NaSO$ the dominant sodium/sulfur product. Measured, —; calculated, O.

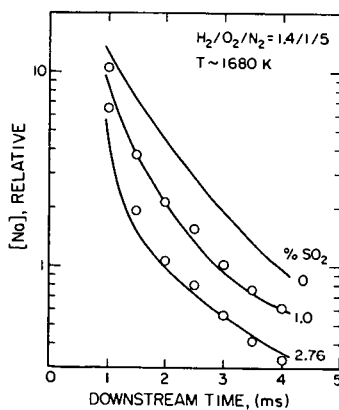


Figure 5. Comparison of measured and calculated sodium profiles in lean $H_2/O_2/N_2$ flames with varying SO_2 and $NaSO_2$ the dominant sodium/sulfur product. Measured, —; calculated, O.